

Author responses to reviewer comments on submission acp-2022-79 ('Investigating the Global OH Radical Distribution Using Steady-State Approximations and Satellite Data') by Pimplott et al.

We would like to thank the reviewers for their useful feedback which will help us to improve our manuscript. We have addressed the specific and general comments from both reviewers and updated the manuscript accordingly. In the table below, we have provided our responses in black text and provided the updated text for the revised manuscript in blue text (subject to edits).

Figures with letter captions e.g. Fig. A, refer to new figures being added into the revised manuscript. Figures with letter captions starting with an S e.g. Fig. SA, refer to figures being added into the revised supplementary material. Figures with number captions starting with R e.g. Fig. R1 refer to figures only in this author response document. Line numbers refer to the original manuscript uploaded to ACP Discussions.

Additional Revisions

In addition to comments from the two reviewers, we have also improved our manuscript in response to other direct comments as summarised below:

Comment	Response
<p>The comment is to revise Eq. (4) (the simplified steady state approximation for OH) to account for water vapour as a sink of O(1D) as follows:</p> $[OH]_{Steady\ State} = \frac{2j_1 k_1 [O_3][H_2O]}{(k_2[N_2] + k_3[O_2] + \textcolor{red}{k_1[H_2O]})} \cdot \frac{1}{(k_4[CH_4] + k_5[CO] + k_6[O_3])}$	<p>We have revised our simplified approximation (Eq. (4)) to include this extra term.</p> <p>In our region of interest (600 – 700 hPa) this has a small effect on our results. We have revised our results and figures in the manuscript accordingly.</p> <p>Closer to the surface (>800 hPa) this has improved the agreement between S-SSA OH and TOMCAT OH compared to that in the original manuscript. However, we do not expect our simplified approximation to capture the complex OH chemistry at the surface. Therefore, we still focus on the mid-tropospheric pressure region of 600 – 700 hPa.</p>

The revision of the results and figures from the additional water vapour sink term and other minor edits are not present in the tracked changes document for the revised manuscript.

Reviewer 1's comments:

General Comments:

"While the authors do spend an appreciable amount of time evaluating the steady state approximation, I'm still left wondering how useful this is in regions that have appreciable OH production from NO. Buried in the supplement is a figure showing that in boreal winter, 2/3 or greater of OH production is from the NO + HO₂ term for most zonal bands in the northern hemisphere. Omitting this from a steady state approximation would undoubtedly lead to incorrect OH values, or at best, correct OH values but for the wrong reason. In comparisons between ATom observations and both the ATom steady state OH and satellite steady state OH, there are multiple points where the steady state approximation dramatically underestimates the observations by a factor of 3 or greater. The reasons for these differences are not clearly articulated but are likely due to the omission of production terms. There is still value in this approach, however, if the authors more clearly show where

secondary production from NO is important in the main text of the paper, and highlight regions where the approximation is likely not to hold."

Thank you for your comments, they are addressed by the specific responses below. In summary, we have added a new section to the revised main manuscript, detailed in comment 11, to address additional terms which could be added to the S-SSA e.g. the NO + HO₂ source term. We add a new figure, Fig. B, to the revised main manuscript to highlight in which regions, the NO + HO₂ source term has a large influence and also new supplement figures SC, SD and SE which show the impact of adding the NO + HO₂ source term to the S-SSA for model and aircraft data.

Specific Comments:

	Comment	Response
1	<p>Paragraph starting on Line 166: <i>Is the simulation discussed in Monks et al (2017) the same as that discussed here? If not, are the two simulations close enough to have similar O3 and CO fields? Similarly, when you say "TOMCAT has a slightly higher global mean tropospheric OH..." are you talking about this simulation explicitly or the one discussed in Monks et al?</i></p>	<p>The simulation discussed in Monks et al. (2017) is not the same as that used in this study. The difference in model set-up, referring to emissions used, is discussed in the previous paragraph (staring line 154). Although the model is fundamentally very similar between the two simulations and we would expect them to produce similar results, there have been a few updates to the TOMCAT model between the Monks et al. (2017) simulations and the ones used in this paper. The version of the model used is more similar to that in Rowlinson et al. (2019), including an update to the cloud field, replacing the climatological cloud fields with reanalyses from ECMWF.</p> <p>The paragraph starting on Line 166 has been re-written to include details of the evaluation of OH made in the Rowlinson et al. (2019) which will be more comparative to the simulation in this study. We have also updated the text to make it clear which simulation we are referring to.</p> <p>"Monks et al. (2017) and Rowlinson et al. (2019) have evaluated TOMCAT OH compared to model and observational datasets for the year 2000. The set-up for the simulations used in Rowlinson et al. (2019) is most similar to that in this study, but broadly the simulation in Monks et al. (2017) produces similar regional zonal OH values. TOMCAT OH in Rowlinson et al. (2019) had an average global tropospheric concentration of 1.04×10^6 molecule cm⁻³, which sits within a range from other studies e.g. $0.94 \pm 0.1 \times 10^6$ molecule cm⁻³ from inferred OH observations from MCF by Prinn et al. (2001), $1.08 \pm 0.6 \times 10^6$ molecule cm⁻³ from the POLARCAT Model Intercomparison Project (POLMIP) and the multi-model mean of $1.11 \pm 0.2 \times 10^6$ molecule cm⁻³ from 16 Atmospheric Chemistry and Climate Model Intercomparison Project (ACCMIP) models (Naik et al., 2013). In terms of vertical distribution, Monks et al. (2017) and Rowlinson et al. (2019) show the maximum TOMCAT OH values to be between the surface and 750 hPa near the equator. In comparison, Spivakovsky et al. (2000) (MCF method) and the multi-model mean OH from ACCMIP (Naik et al., 2013) have peak OH values higher up in the troposphere. Overall, in the mid-troposphere, the primary focus in this study, Rowlinson et al. (2019) TOMCAT OH shows comparable values across all the latitude regions in comparison with Spivakovsky et al. (2000) and ACCMIP (Naik et al., 2013)."</p>
2	<p>Line 207: <i>Please indicate the sign of the bias (i.e. The satellite is high by</i></p>	<p>The bias is positive, with the satellite being larger by up to 20 %. This has been clarified in the manuscript.</p>

	<i>up to 20%). The current wording is ambiguous.</i>	<i>"When compared with ozonesondes (Supplementary Sect. S3), O₃ retrieved in the mid-troposphere by the IMS-extended scheme is found to be systematically larger by up to 20 %."</i>
3	Figure S5: <i>It would be helpful to have a legend on the figure itself indicating what color corresponds to which observation, instead of just having this information in the figure caption.</i>	A legend has been added to the figure and the revised figure is shown in Figure SA.
4	Line 221: <i>Is this just the global average? It looks like there could be significant variation in this value, but it is hard to judge that from comparing Figures 2 and S6. A map showing the percent uncertainty, instead of the absolute value, might be more useful.</i>	We found that the monthly averages for the percentage uncertainty for each grid-box was fairly consistent, with the uncertainty ranges from 23–24 %, as shown in Fig. R1. Therefore, we decided to use the absolute values instead.
5	Section 2.3.3: <i>What's the time resolution of the ATom observations?</i>	We have used ATom observations that are merged into an average of 2-minute sample interval. We have added this detail into Section 2.3.3. <i>"Wofsy et al. (2018) merged the observations into a two minute sampling interval."</i>
6	Line 248: <i>I think you need a more thorough comparison between the TOMCAT OH and the SS approximation. Just looking at zonal means is likely obscuring regional effects, particularly because NO contributions to OH production are likely to be more important over land than over the remote ocean, even at 600 – 700 hPa. Some of this can be discerned from Figure 3, but there should be more discussion about the regional differences in agreement. Figures showing the absolute or relative difference between TOMCAT and the SS approximation would be appropriate as would a regression.</i>	Figure A shows the difference between TOMCAT OH and S-SSA using model and satellite data. We have added a discussion of the regional differences in agreement into Sect. 3.2.1. <i>"Figure A shows the spatial differences between the TOMCAT and S-SSA OH. In January, the S-SSA shows an underestimate of up to $\sim 2 \times 10^6$ across the Northern Hemisphere and over parts of the oceans across the Southern Hemisphere, mostly between the equator and 30°S e.g. the Atlantic, edges of the Pacific, but not the Indian Ocean. In the Southern Hemisphere, an overestimate is present over some of the continents, e.g. up to $\sim +2 \times 10^6$ molecule cm⁻³ in S America, and up to $\sim +1 \times 10^6$ molecule cm⁻³ in the Indian Ocean and the centre of the Pacific. Broadly, the peak [OH] values across SE Indian Ocean and S African continent show good agreement.</i> <i>In June, the S-SSA shows good agreement over the oceans in the NH, mostly between the equator and 30°N, and the S American and Australian continent in the SH. An overestimate of up to $\sim +4 \times 10^6$ is found across the peak [OH] values found across the N African continent and China. A slight underestimate of up to $\sim -1 \times 10^6$ is found on landmasses around the equator.</i> <i>In summary, the S-SSA agrees with TOMCAT across the oceans near the equator, depending on the season. The peak values of [OH] are found in similar locations for TOMCAT and S-SSA [OH], however, the S-SSA generally produces an underestimate at these peak values."</i>
7	Table 1 and throughout the text: <i>Are you using mass-weighted OH when you're making your global</i>	All global/regional OH means throughout the text are mass-weighted. We have clarified this in the manuscript.

	<i>comparisons? If not, you should be, otherwise you're likely giving too much importance to regions that don't particularly matter.</i>	
8	<i>Line 287: How accurate is your model JO1D? CAM-Chem, for example, has a notable low bias in JO1D in the altitude range you're examining (Nicely, et al, 2016). In your uncertainty analysis, you assume there is no error in JO1D, but that is highly unlikely. If you don't know how accurate the modelled JO1D is, you should add a sentence or two at least noting that this is a potential source of error.</i>	<p>We believe that our model j_{O_3} is reasonable, as we have compared it to ATom observations of j_{O_3}, which is shown in Fig. SA.</p> <p>This comparison has the same issues, of comparing model and aircraft observations, as discussed in your comment 13 and the response. Figure SB shows that TOMCAT j_{O_3} has a negative mean bias (TOMCAT is lower than ATom observed j_{O_3}) across the 4 campaigns, ranging from -0.09 to $-1.29 \times 10^{-5} \text{ s}^{-1}$. There are notable areas of disagreement, such as near the equator in ATom-2, between 60°S and 20°S in ATom-3, between the equator to 20°N in ATom-4 and between 40°N to 60°N in ATom-4.</p> <p>We have added a sentence into the main manuscript and also into Section S5 (with Fig. SB), acknowledging that this is a potential source of error.</p> <p><i>"This assumes that there is no uncertainty in the rate constants (j_1, k_{1-6}), which is a potential source of error."</i></p>
9	<i>Line 305: What's the r2 value for a regression of the satellite and model OH?</i>	The correlation co-efficient between the monthly average grid-boxes of satellite OH and model OH is 0.82 for January and June. The r^2 value is 0.68 for both months. We have added this detail into section 3.1.2.
10	<i>Line 309: You're missing a period after "18%".</i>	We have added this in.
11	<i>Line 311: Is this missing peak in North America likely due to the omission of a NOx term in your SS approximation? I think either here or elsewhere, there needs to be a more explicit discussion of how omitting NO and VOC sinks likely limits the accuracy of your satellite SS product in certain regions. Maps showing the relative importance of NO to OH production and the other VOCs to OH loss could help illustrate where this product will likely have more limitations, or bringing a subset of the panels from Figures S9 and 10 to a main figure could be helpful.</i>	<p>We have added a new section (Sect. 3.1.X) which details our findings of which reactions are important to the OH approximation throughout the troposphere, and how this limits the accuracy of our satellite S-SSA product in different regions.</p> <p><i>"3.1.X Study of reactions omitted from the S-SSA</i> <i>The aim of this study is to derive information about OH from satellite data, therefore some source and sink reactions, which don't have relevant satellite retrievals, have been omitted from the S-SSA. We apply TOMCAT model data to another more complex steady-state approximations, Sav-SSA, to demonstrate which atmospheric species additional to H_2O, O_3, CO and CH_4 are key to OH production and removal in the pressure ranges, <400 hPa and >800 hPa. The results are shown as zonal means in supplement Sect. S7. Figures S9 and S10 show that the reaction of nitric oxide (NO) and the hydroperoxy radical (HO_2) to be an important missing source at pressures <400 hPa. The OH and HO_2 radicals are closely linked in chemical cycles which are not, however, represented in the S-SSA.</i></p> <p><i>Figure B shows the regional impact of the $\text{NO} + \text{HO}_2$ source term on the total production term of the Sav-SSA, averaged across the 600 – 700 hPa pressure layer. For January, the $\text{NO} + \text{HO}_2$ source term shows a very large percentage contribution between 30°N and 60°N (up to 100%), although the [OH] is very low here. In areas with very high $\text{NO} + \text{HO}_2$ percentage contributions, it is likely that the S-SSA is not sufficiently capturing all the important chemical pathways. Below 30°N, the spatial distribution of this percentage contribution is similar to the spatial distribution of the</i></p>

negative differences between TOMCAT and S-SSA [OH] in Fig. A, indicating that these regions could indeed have improved agreement with the addition of this source term. For example, across the NH oceans and continents and in the SH Atlantic and Pacific Ocean off the coast of S America. For June, the $\text{NO} + \text{HO}_2$ source term makes a larger percentage contribution across the SH oceans and continents (where [OH] is low). In the NH, the $\text{NO} + \text{HO}_2$ source term makes a greater contribution over land, and a very low contribution over the oceans, where Fig. A shows that the S-SSA [OH] is in good agreement with the TOMCAT [OH].

Figures SC and SD show a comparison between [OH] calculated using the S-SSA, as in Eq. (4), and with the addition of 1 source term ($\text{NO} + \text{HO}_2$) and 2 sink terms ($\text{NO} + \text{OH} + \text{M}$ and $\text{NO}_2 + \text{OH} + \text{M}$). The [OH] calculated using the NO_x terms shows an overestimate of between ~ 0 and 4×10^6 molecule cm^{-3} compared to TOMCAT [OH] for both January and June 2010 and improves the agreement in some regions, such as at broadly above the equator in January and below the equator in June.

Although the $\text{NO} + \text{HO}_2$ source term is important in some regions, there are no NO or HO_2 satellite observations available in the relevant pressure range, so we cannot include this term in the S-SSA in this study. This is an area for potential future work, to introduce co-located tropospheric NO_2 satellite data from another instrument on MetOp, the Global Ozone Monitoring Experiment-2 (GOME-2), alongside IASI (Munro et al., 2016). This would require additional steady-state balance expressions for $\text{NO}:\text{NO}_2$ and for HO_2 .

The current source term, photolysis of ozone and subsequent reaction of the photo-generated $\text{O}^{(1)\text{D}}$ atoms with H_2O , is controlled above the tropopause by the amount of H_2O , which is much lower than in the troposphere. The omission of the other, more dominant, sources of OH in the S-SSA above the tropopause yields an underestimation in OH.

Figure C shows the regional impact of two VOC terms (of interest) on the total production term of the Sav-SSA, averaged across the 600 – 700 hPa pressure layer. The regional contribution of all sink terms can be found in the supplementary material. Figure C shows that C_5H_8 (isoprene), from the sum of hydrocarbon term, shows a large contribution across South America and Indonesia in both January and June. These are regions of high S-SSA OH compared to TOMCAT OH seen in Fig. A, representing the lack of this sink term in the S-SSA, leading to an overestimation by the S-SSA. In these regions, the S-SSA expression is shown to not fully capture the OH chemistry. Formaldehyde (HCHO) represents $\sim 10\%$ of the total sink term in both months.

These additional source and sink terms could potentially help reduce the overestimate of the S-SSA in this region. Satellite data on tropospheric columns of NO_2 and several other relevant species (HCHO and SO_2 at enhanced levels) are available from GOME-2 alongside IASI on MetOp. Other than in tropical regions of lightning NO_x production and rapid convective uplift, these reside principally in the lower troposphere. Co-

		<p>located data from GOME-2 could therefore allow further investigation in future work. For the other source and sink species, satellite data is not available in the relevant pressure region or not available from a similar instrument to the species in the S-SSA which would yield problems, such as in combining observations with different vertical resolutions at different locations and times of day.</p> <p>Overall, the spatially varying importance of different source and sink terms prevents the S-SSA from achieving a spatially uniform agreement and this must be considered when applying the approximation."</p>
12	<p>Line 325: More discussion of why agreement is significantly degraded for ATom 2 as compared to the other campaigns is needed. Also, for each of the campaigns there is almost a second trend line, where observed OH ranges up to 10×10^6 molecules/cm³ but the SS approximation doesn't exceed 1. What is driving the poor agreement for these points? Does agreement improve if you include an NO term in the SS approximation?</p>	<p>Broadly, we believe that ATom-2 shows the poorest agreement for a normalised mean bias due to the predominance of smaller values of [OH] for both OH-calc and OH-obvs, which leads to a higher percentage difference, although for absolute difference (mean bias) ATom-2 does not have the largest values. We have added this discussion of why the agreement for ATom-2 might be degraded in Sect. 3.1.3.</p> <p>We have added a new section (Sect. 3.1.4) detailing the implication of adding NO_x into the OH-calc for the ATom observation comparison.</p> <p>"In Fig. SE we show a version of Fig. 4, as a comparison of ATom OH-calc with (OH-calc-NO_x) and without (OH-calc) 3 NO_x reactions (NO + HO₂, NO + OH + M, NO₂ + OH + M) included in the S-SSA). The addition of the NO_x terms changes the bias in the OH-calc relative to OH-obvs from -20.6 % to +13.2 %. This change in sign is consistent with the comparison of S-SSA and S-SSA with NO_x reactions using model data as shown in Figs. SC and SD. Overall the correlation stays similar for with and without NO_x (0.76 and 0.78). This corresponds to the model results in Sect. 3.1.X which find that for some regions, the NO + OH₂ source term can make a large contribution to the total source term."</p> <p>For the 'second trend line', the higher values of OH-obvs (with OH-calc still < 1) e.g. in ATom-3,4 are not improved much by the addition of NO_x to the approximation. In general, for the lower OH values, the addition of NO_x does improve the agreement, apparent across the 4 campaigns.</p>
13	<p>Line 359: What is the horizontal extent of the OH observations and how does this compare to the satellite product resolution? Is the horizontally homogeneity of OH enough to allow for a comparison to a satellite product at 3 degree resolution?</p>	<p>In comparison with the model and satellite data, the ATom data has very limited horizontal sampling. The horizontal extent ranges from ~180°W to ~20°W across the four campaigns. Therefore this is limited to West of the Greenwich Meridian, and mostly focused on covering the Pacific and Atlantic Oceans.</p> <p>Unfortunately there is a lack of other direct in-situ measurement datasets to compare our satellite-derived OH to, so comparison to the ATom data is definitely worthwhile in our view, despite the challenging comparison due to the very different horizontal sampling and coverage of the dataset.</p> <p>OH has a short lifetime and so it is unlikely that the ATom measurements will show enough horizontal homogeneity to be directly compared to the grid-box averaged data. Therefore, we have displayed the data in Fig. 5 in a way which takes this into account, overlaying the ATom point data on top of the OH field underneath to highlight the issue with the comparison.</p>

		<p>We believe that it is worth presenting this data, but we have added in a sentence in Sect. 3.1.3 to further highlight and detail the issues with this comparison.</p> <p>“The comparison is challenging due to the sparse nature of the ATom data points compared to the satellite [OH] field (highlighted in Fig. 9) and using data only for 2017 (ATom-1 was from 2016 and ATom-4 from 2018). The poor comparison in some regions may be attributable to the resolution difference between the point aircraft observations and the averaged satellite [OH] field, due to the lack of horizontal homogeneity of OH.”</p>
14	<p>Figure 7: This figure highlights the poor performance in the 30 – 90 N range. Figure S9 likely suggests part of the reason, since, according to TOMCAT, greater than 2/3 of the OH production is from the NO + HO₂ reaction. Again, more discussion is needed as to how this limits the applicability of your product to regions with appreciable secondary OH production from NO.</p>	<p>We have now discussed the implications of NO_x in response number 11 in this document, and in new Sect. 3.1.X. We have added a sentence into Sect 3.1.3 to relate this to our NO_x results in Sect. 3.1.X.</p> <p>“This corresponds to the results in Sect. 3.1.X, where the OH source reaction HO₂ + NO represents a larger contribution to the total production in the Northern high latitudes in the Northern Hemisphere winter (ATom-2,3,4). The reduction in agreement in this region, indicates that the S-SSA may not be able to provide robust information about [OH] here region. In Sect. 3.3 we study a tropical (15° S–15° N) band, where the S-SSA shows a more robust agreement.”</p>
15	<p>Line 391: How much does the stratospheric O₃ column in your model vary between 2008 and 2017? How would any trends or internal variability affect your JO1D and consequently your OH calculation?</p>	<p>The TOMCAT model simulations use a climatological stratospheric ozone field so there will be no variation in its stratospheric ozone column between 2008 and 2017. In our study of the long-term variability of S-SSA OH, we use a fixed year of photolysis rates from model year 2010, which removes any influence of varying photolysis rates on the variation in the calculated OH. This assumption should be considered when interpreting our results, and therefore we have added in a sentence (to Sect. 3.1) to highlight this. An attempt to model the variation in stratospheric O₃ (and consequently j_1) is beyond the scope of the study at present, though it is a potential item to address in further work, as satellite observations would be available too.</p> <p>“We use satellite data produced on a sub-sampled basis from 2008–2017 and the S-SSA, together with fixed monthly model j_1 distributions from the TOMCAT model for a fixed year (2010). The use of a fixed year of j_1 distributions removes any influence from variation in this value between years e.g. from variation in stratospheric ozone, which is an assumption that should be considered when interpreting these results.”</p>

Reviewer 2's comments:

General comments:

“This is a very interesting and novel idea that is worth publication in ACP once several deficiencies (listed below) have been addressed.”

Thank you for your comments.

Specific comments:

	Comment	Response
1	Minor comment: Line 51: <i>In situ measurements are scarce also as it's not a simple measurement. There aren't very many OH instruments and they certainly aren't commercialized yet.</i>	<p>We have added this in.</p> <p>"Direct in situ measurements of OH are scarce as the measurement process is challenging with few instruments available (Stone et al., 2012; Lelieveld et al., 2016). Due to its very short lifetime, ~1 second in the daytime, the abundance of OH is very low with the global tropospheric mean OH concentration is around 1×10^6 molecule cm⁻³."</p>
2	Major concern: Line 279-285: <i>What are the implications of these conclusions for your ability to use satellite observations to constrain OH? I would expect that you could devote an entire section to this discussion.</i>	<p>We have written a new section (Sect. 3.1.X) to discuss the results of our study of which reactions are important in the approximation of OH in the atmosphere and also the pressure range of interest, 600-700 hPa.</p> <p>Please see the response to comment 11 from Reviewer 1.</p>
3	Major concern: Line 287: <i>Just how much of the tropospheric burden of OH resides between 600 and 700 hPa? How important is this layer for the tropospheric oxidation of methane and other trace gases? That is, can you give an idea of how much of the troposphere's oxidizing capacity that you can constrain from space? Even if the answer is "not much", I still believe that your paper represents a great first attempt to indirectly constraining OH using space-borne observations of the species that influence OH.</i>	<p>We found that the 600-700 hPa pressure region contributed to ~15 % of the tropospheric OH burden, and ~19 % of the burden weighted to methane oxidation. This is detailed in Sect. 3.1.1.</p>
4	Major concern: Figure 2: <i>Can you discuss how cloudiness affects your sample number and, subsequently, your uncertainties? What are the other limitations of satellite data for your purposes?</i>	<p>We have added in the following to Sect. 2.3.2 to discuss the impact of cloudiness on sample number and uncertainties.</p> <p>"Co-located retrievals of H₂O, O₃ and CO data and CH₄ were filtered for a geometric cloud fraction of 20% or less (i.e. 0.2 fractional coverage or less). This resulted in satellite soundings which exclude all opaque clouds which fill the field of view and a fraction of clouds which fill part of the field of view. In comparison with TOMCAT, which had no filtering for cloud, this could produce a clear skies bias. However, the model is driven by ECMWF meteorological fields, which are also used in the satellite retrieval, so they should be reasonably consistent.</p> <p>Figure SE shows the daily average number of retrievals used per grid box for the calculation of satellite [OH]. Globally, the daily average number of grid-box profile retrievals for the input species ranges between 0 and 24, with an average of ~6. Therefore, there are sufficient retrievals of the trace gases in the S-SSA to calculate values of OH for most grid-boxes every day."</p>

		For the other limitations of satellite data for our purpose, a key limitation inherent to the satellite data is the different vertical sensitivities of H ₂ O, O ₃ , CO and CH ₄ retrievals as represented by their respective averaging kernels. This is discussed in Sect. 2.3.2 and Sect. S3 and papers referenced. These satellite data on H ₂ O, O ₃ , CO and CH ₄ have been evaluated in earlier studies and estimates of their accuracies were provided in Sect. 2.3.2 and Sect. S3.
5	Major concern: Line 336: <i>This is a bold statement given the limited spatiotemporal extent of the OH observations. For example, do you expect your SSA to compare well over and downwind of continents where air is more polluted?</i>	<p>Figure R2 shows the absolute difference between OH-calc and OH-obvs at the location of the ATom observation. Broadly there does not seem to be a strong relationship between the difference and being over/downwind of continents where you would expect to find more polluted air across all 4 campaigns. For example, ATom-1,3 find higher differences across the N American continent, but ATom-2,4 do not.</p> <p>We filter the data for air influenced by biomass burning (acetonitrile concentration > 200 ppt), so this could contribute to the lack of relationship.</p> <p>We have re-written this statement to account for the limited spatiotemporal extent of the ATom OH observations.</p> <p><i>"The normalised mean bias between OH-obvs and OH-calc is ~26 % which is a similar order of magnitude to the large uncertainty of 35 % for the OH observations. The ATom observations provide a comparatively large dataset for comparison, however, it has a limited spatiotemporal extent, which should be considered when interpreting our results. Here, we believe that for the observations studied, the datasets are correlated sufficiently to justify further study of the S-SSA at this pressure range."</i></p>
6	Line 457: <i>What about the issue of cross-correlations? Are many of the drivers of ozone concentrations also the drivers of OH concentrations? Would you expect the same result if you had, for instance, NOx in your SSA equations?</i>	We acknowledge that cross-correlations will likely exist between O ₃ and OH as they are linked closely through their chemical reactions. We will add in a brief mention of this possibility in the text at this point. However, a detailed analysis and quantification of this is beyond the scope of our study.

Figures

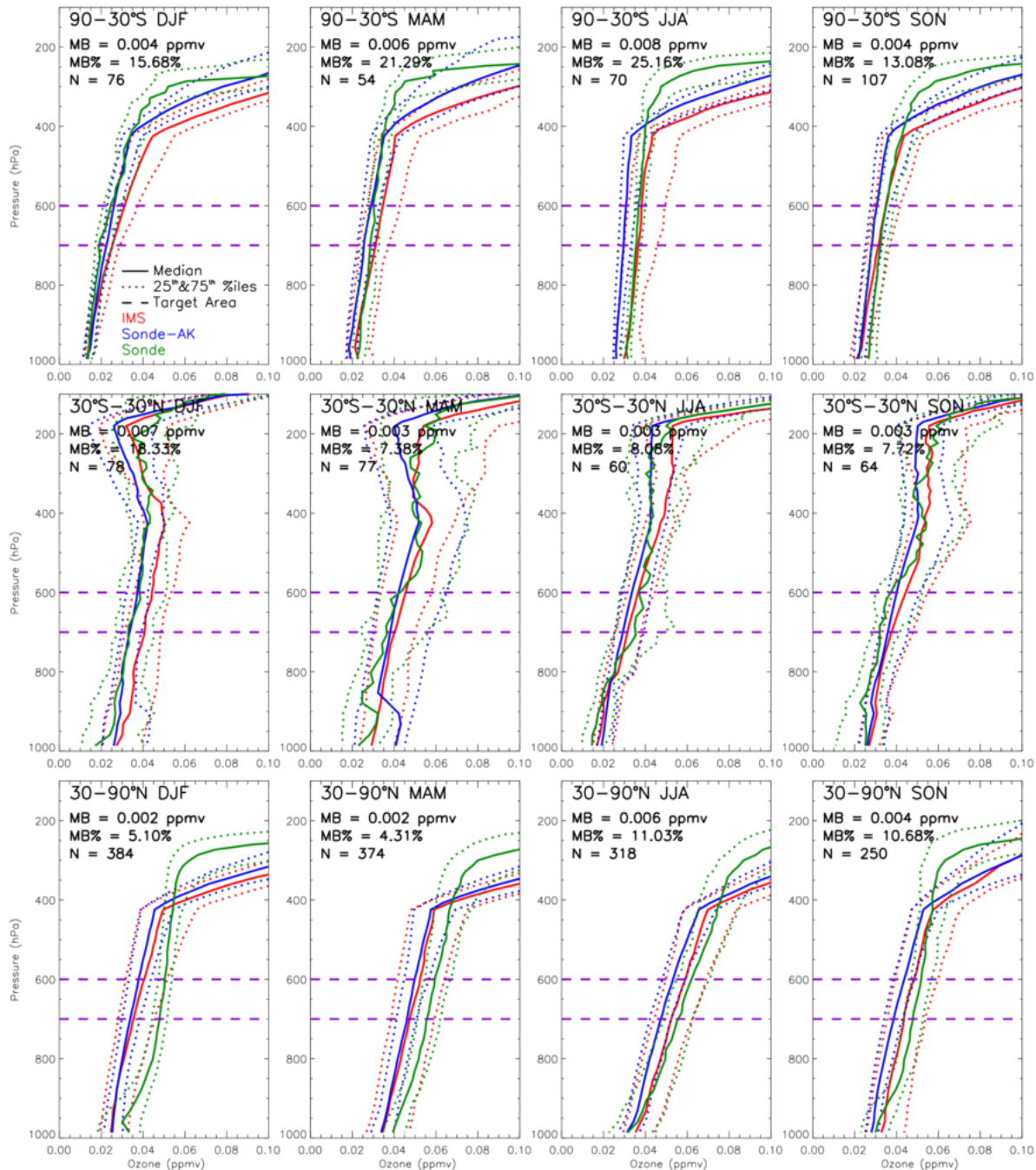


Figure SA: Comparison of ozone profiles retrieved by the IMS scheme with ozonesonde (WOUDC and SHADOZ) profiles (ppmv) for 2010 and 2017 merged. The regions are split into three latitude bands (90–30°S, 30°S–30°N & 30–90°N) and four seasons (December–January–February (DJF), March–April–May (MAM), June–July–August (JJA) & September–October–November (SON)). Red, blue and green solid (dotted) profiles show the median (25th and 75th percentile) IMS, ozonesonde with IMS averaging kernels applied and ozonesonde profiles. Here, the closest satellite retrieval within 500 km and 6 hours of each ozonesonde profile has been used. The purple dashed lines represent the pressure region of interest (600–700 hPa). The mean bias (MB), percentage bias (MB%), and number of sonde profiles (N) are shown based on the 600–700 hPa segments of the profiles.

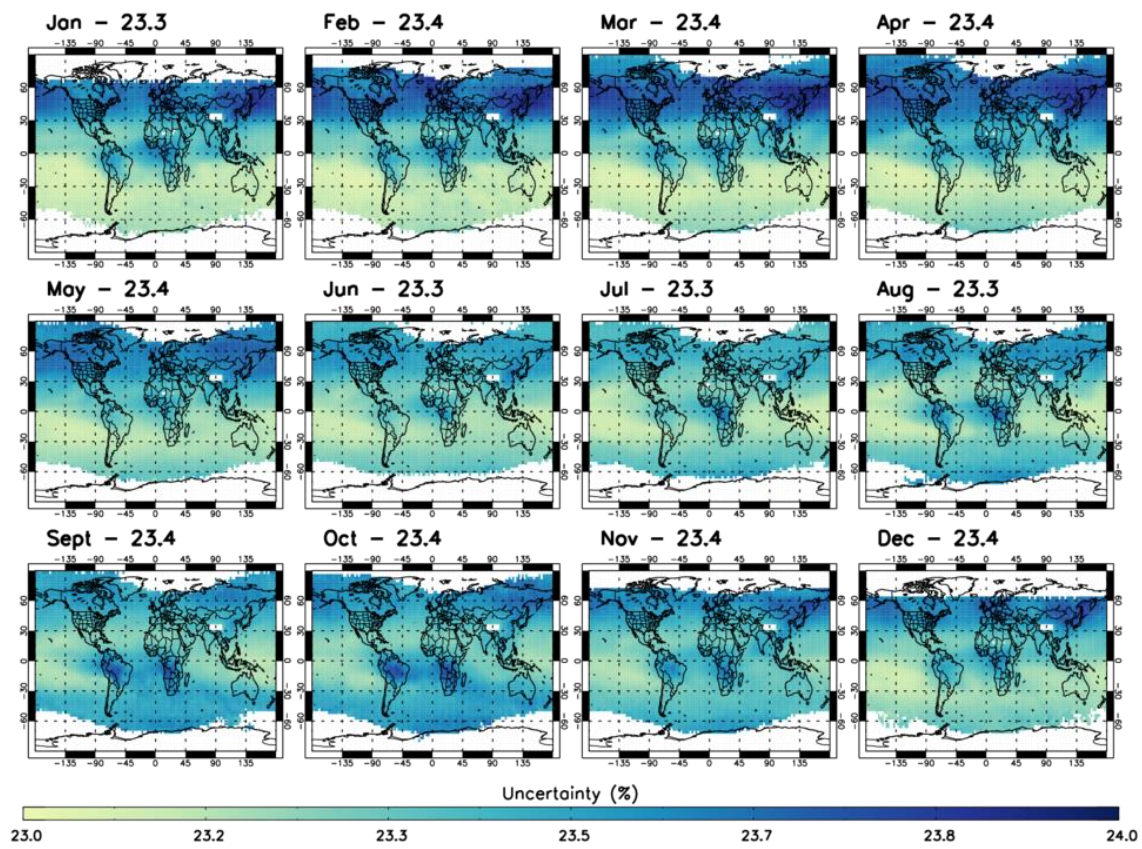


Figure R1: Estimated percentage uncertainty for satellite S-SSA OH for all months of 2010.

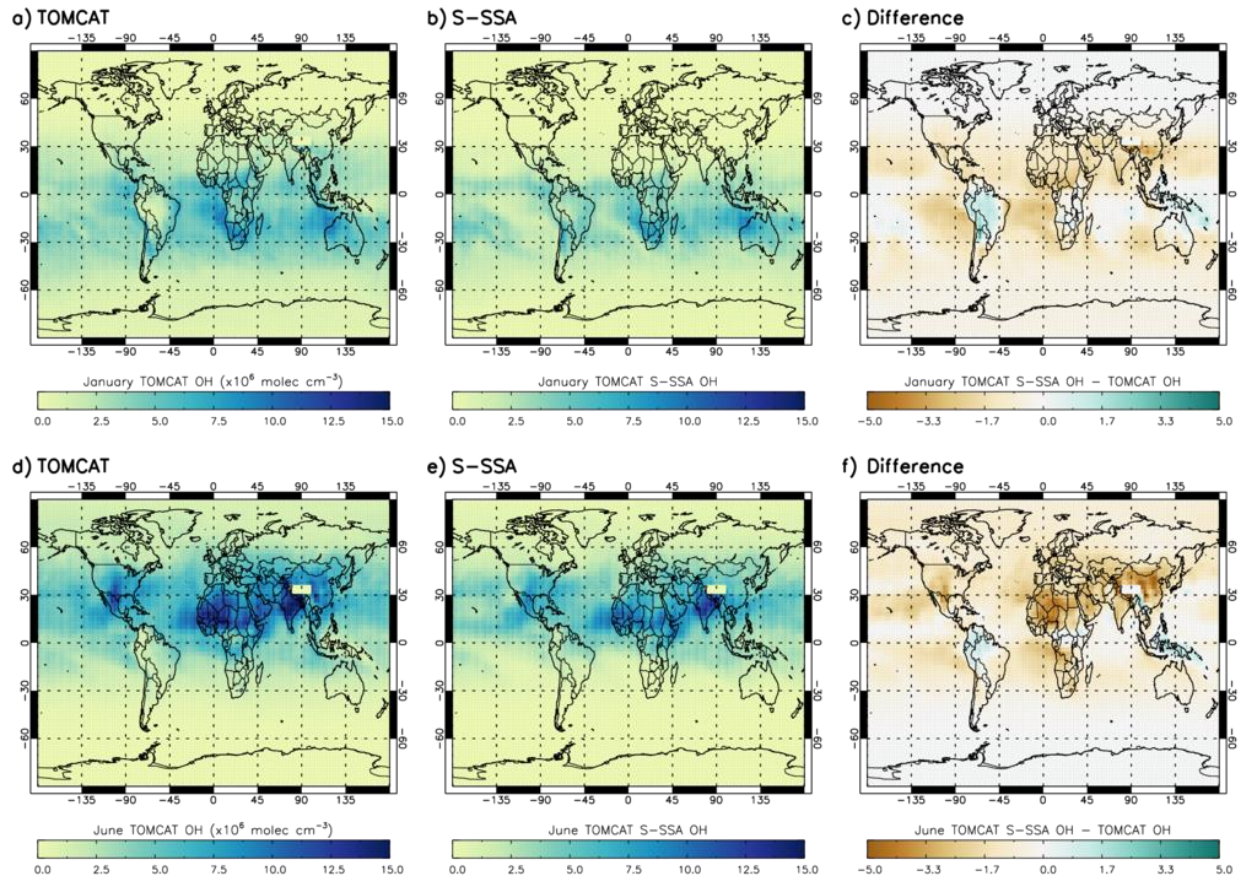


Figure A: OH concentrations averaged over the 600-700 hPa range for TOMCAT, S-SSA and the difference (TOMCAT S-SSA minus TOMCAT). Panels a)-c) and d)-f) represent comparisons for January and June, respectively. All values are in units of $\times 10^6$ molecule cm^{-3} .

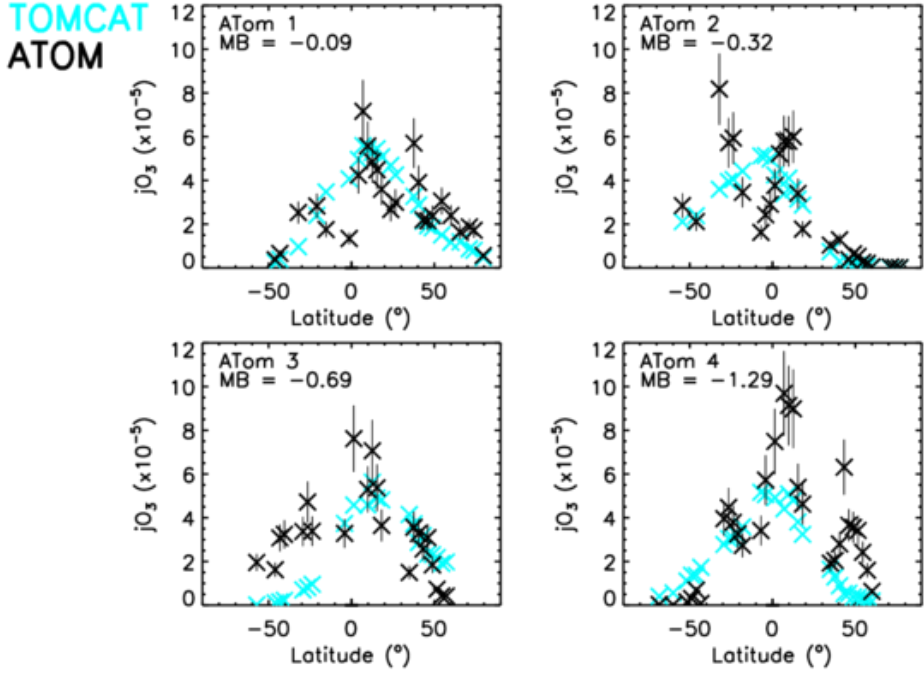
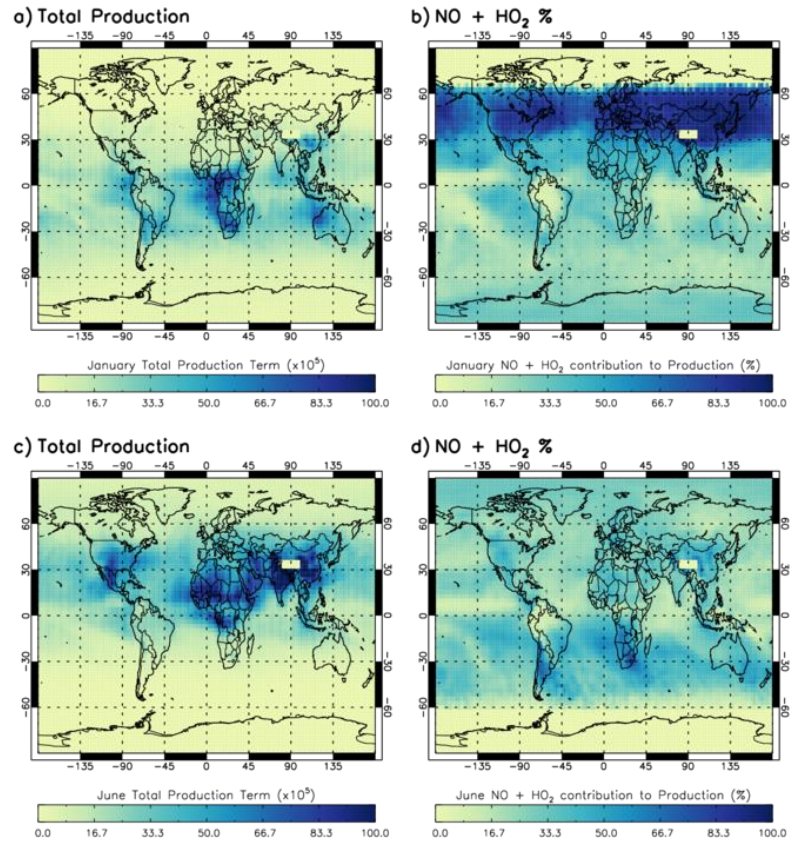


Figure SB: Comparison between TOMCAT j_{O_3} values and ATOM j_{O_3} observations, averaged for each model latitude bin. The four panels show the data split into the individual campaigns. ATOM observations are filtered for 600–700 hPa and 08:00–11:00 LT. All data is in units of $\times 10^{-5} \text{ s}^{-1}$. The mean bias (calculated from TOMCAT - ATOM) are displayed in the top left corner of each panel. Error bars of $\pm 20\%$ (representing the instrument uncertainty (Shetter and Müller, 1999)) are displayed for each ATOM observation .

Figure B: Contribution of $\text{NO} + \text{HO}_2$ reaction to total production term for Sav-SSA in 2010 averaged for the 600-700 hPa pressure region. (a) total production term in January, (b) percentage contribution of the $\text{NO} + \text{HO}_2$ source reaction to the total production term in January, (c) total production term in June, (d) percentage contribution of the $\text{NO} + \text{HO}_2$ source reaction to the total production term in June. Total production is in units of $\times 10^5 \text{ molecule cm}^{-3} \text{ s}^{-1}$.



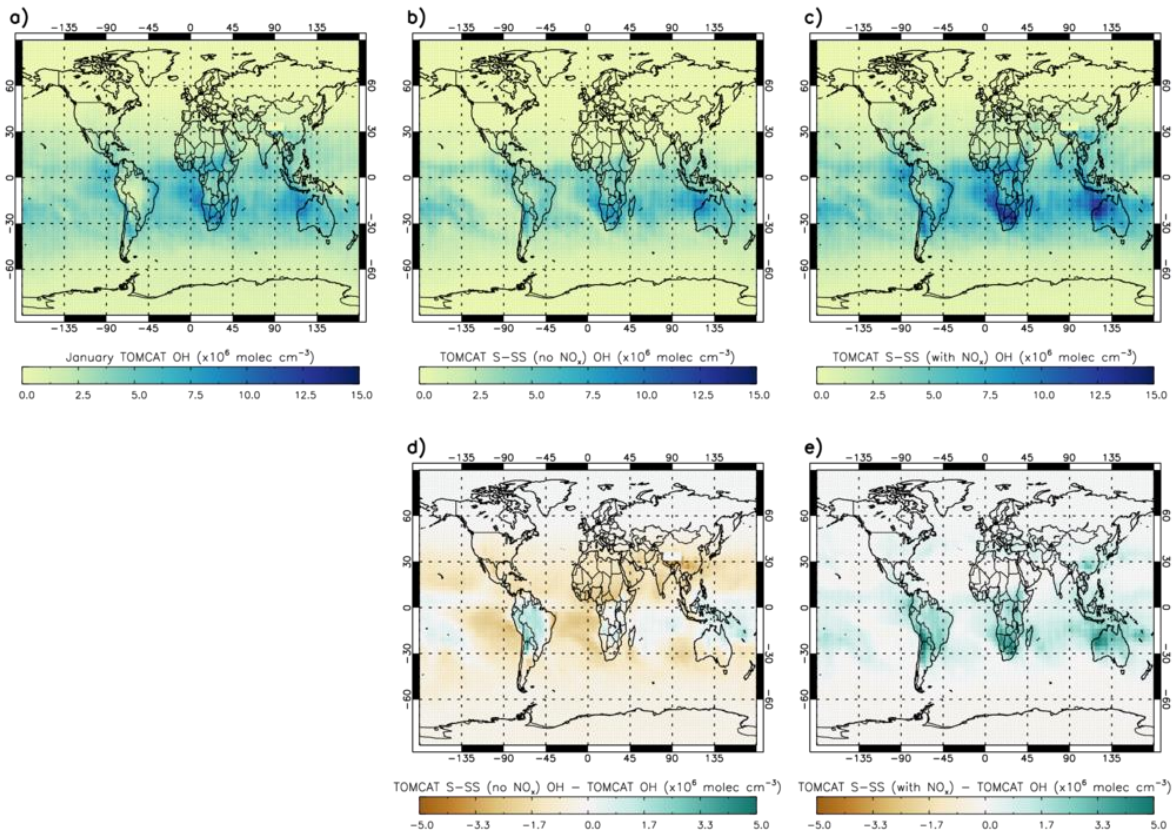


Figure SC: 2D plots of (a) TOMCAT [OH], (b) S-SSA [OH], (c) S-SSA with NOx sources/sinks (NO + HO₂, NO + OH + M, NO₂ + OH + M), (d) difference between S-SSA [OH] and TOMCAT [OH] and (e) difference between S-SSA [OH] with NOx sources/sinks and TOMCAT [OH]. All averaged for the 600-700 hPa pressure region for January in 2010. All values are in units of $\times 10^6$ molecule cm⁻³.

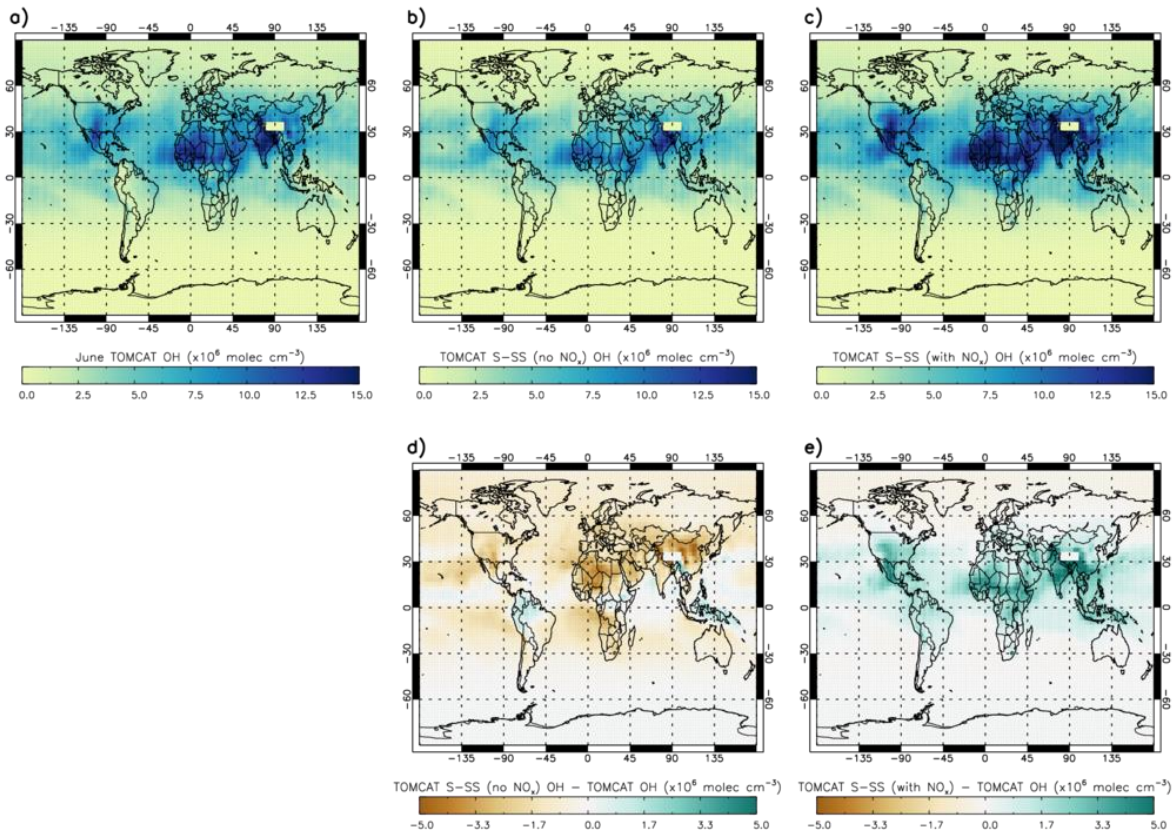


Figure SD: 2D plots of (a) TOMCAT [OH], (b) S-SSA [OH], (c) S-SSA with NOx sources/sinks ($\text{NO} + \text{HO}_2$, $\text{NO} + \text{OH} + \text{M}$, $\text{NO}_2 + \text{OH} + \text{M}$), (d) difference between S-SSA [OH] and TOMCAT [OH] and (e) difference between S-SSA [OH] with NOx sources/sinks and TOMCAT [OH]. All averaged for the 600-700 hPa pressure region for June in 2010. All values are in units of $\times 10^6 \text{ molecule cm}^{-3}$.

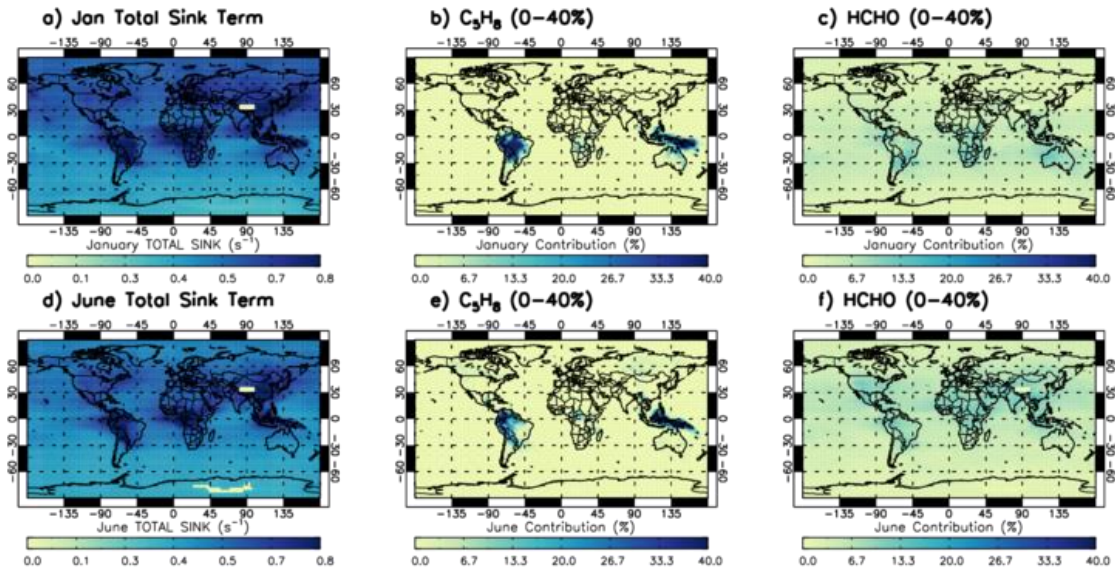


Figure C: Contribution of isoprene (C_5H_8) and formaldehyde (HCHO) OH sink reactions to the total sink term for Sav-SSA in 2010 averaged for the 600-700 hPa pressure region. (a) Total sink term in January, (b) percentage contribution of the $OH + C_5H_8$ to the total sink term in January, (c) percentage contribution of the $OH + HCHO$ to the total sink term in January, (d) total sink term in June, (e) percentage contribution of the $OH + C_5H_8$ to the total sink term in June, (f) percentage contribution of the $OH + HCHO$ to the total sink term in June. Percentage value in panel label (i.e. 0-40 %) refers to the colour bar range. Total sink is in units of s^{-1} .

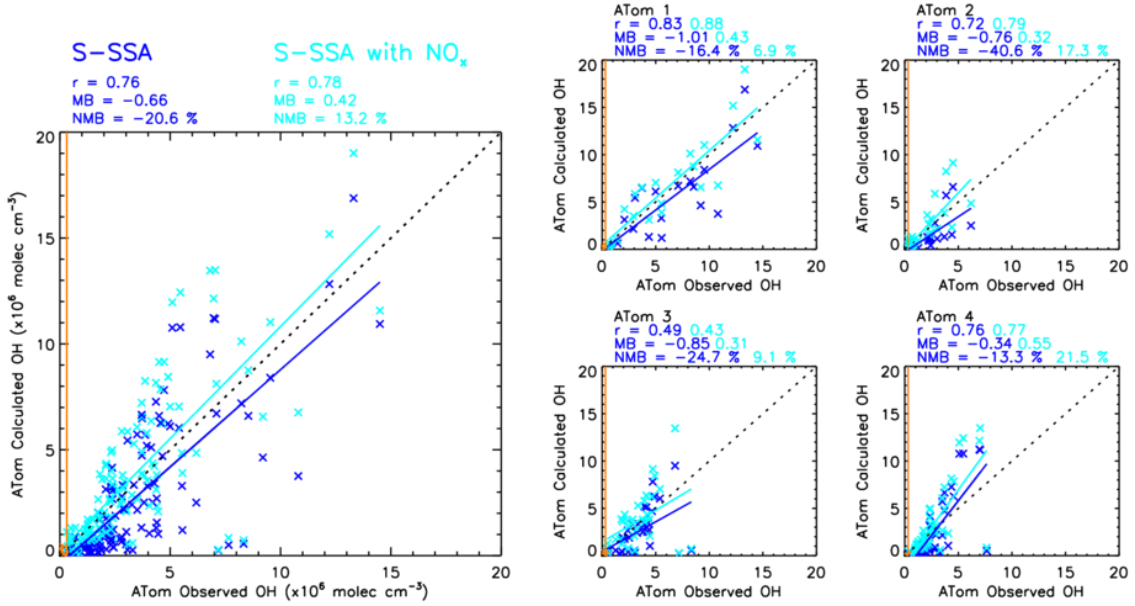


Figure SE: Comparison between OH-calc and OH-obvs for the S-SSA with and without NO_x reactions (NO + HO₂, NO + OH + M, NO₂ + OH + M). The left panel shows a combination of ATom-1, ATom-2, ATom-3 and ATom-4. The right four panels show the data split into the individual campaigns. ATom observations are filtered for 600–700 hPa and 08:00–11:00 LT. All data is in units of $\times 10^6$ molecule cm⁻³. Data points in orange are excluded from the analysis, either as an outlier ($>$ mean + 3.0 standard deviations) or below the limit of detection of the ATHOS instrument (0.018 pptv or 0.31×10^6 molecule cm⁻³) shown by the orange line. Pearson's correlation co-efficient (r), the mean bias (calculated from OH-calc – OH-obvs) and the normalised mean bias (% with respect to OH-obvs) are displayed in the top left corner of each panel.

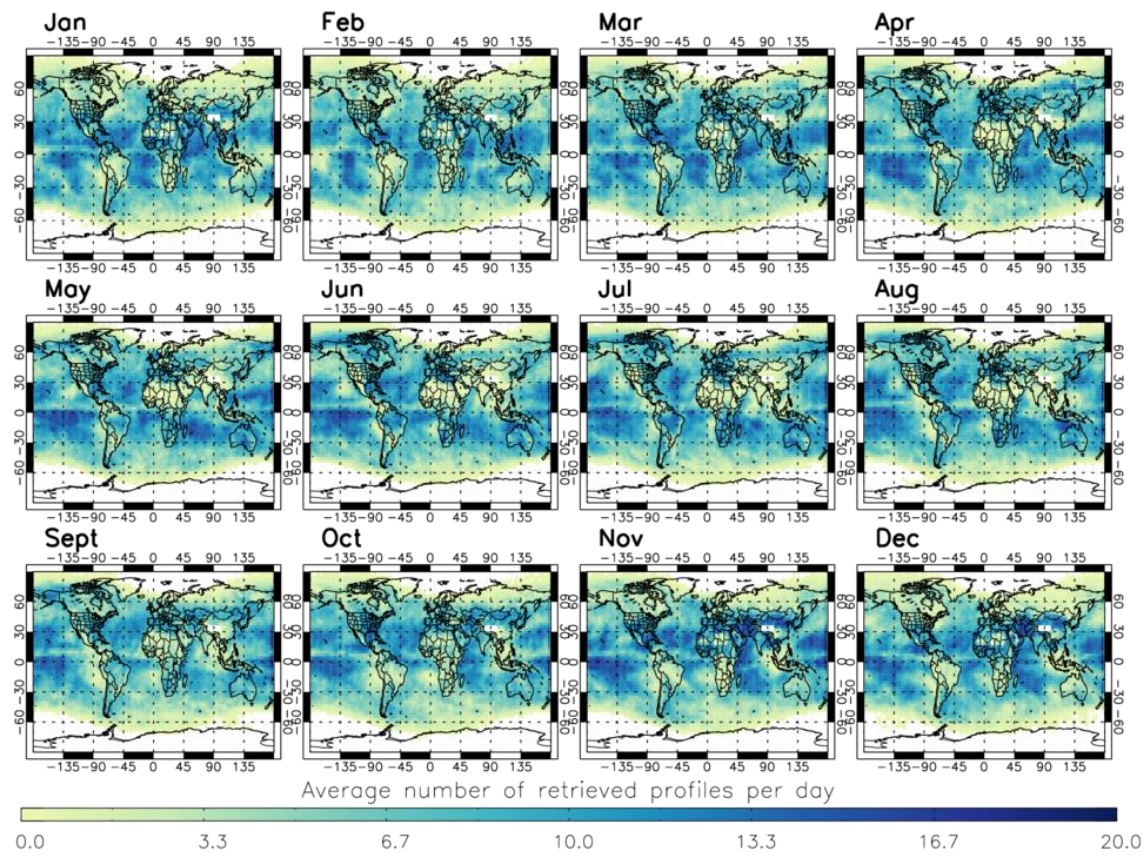


Figure SF: Average daily number of retrieved profiles of the input species (O_3 , CO , CH_4 & H_2O) used in OH calculation for each grid box for each month in 2010.

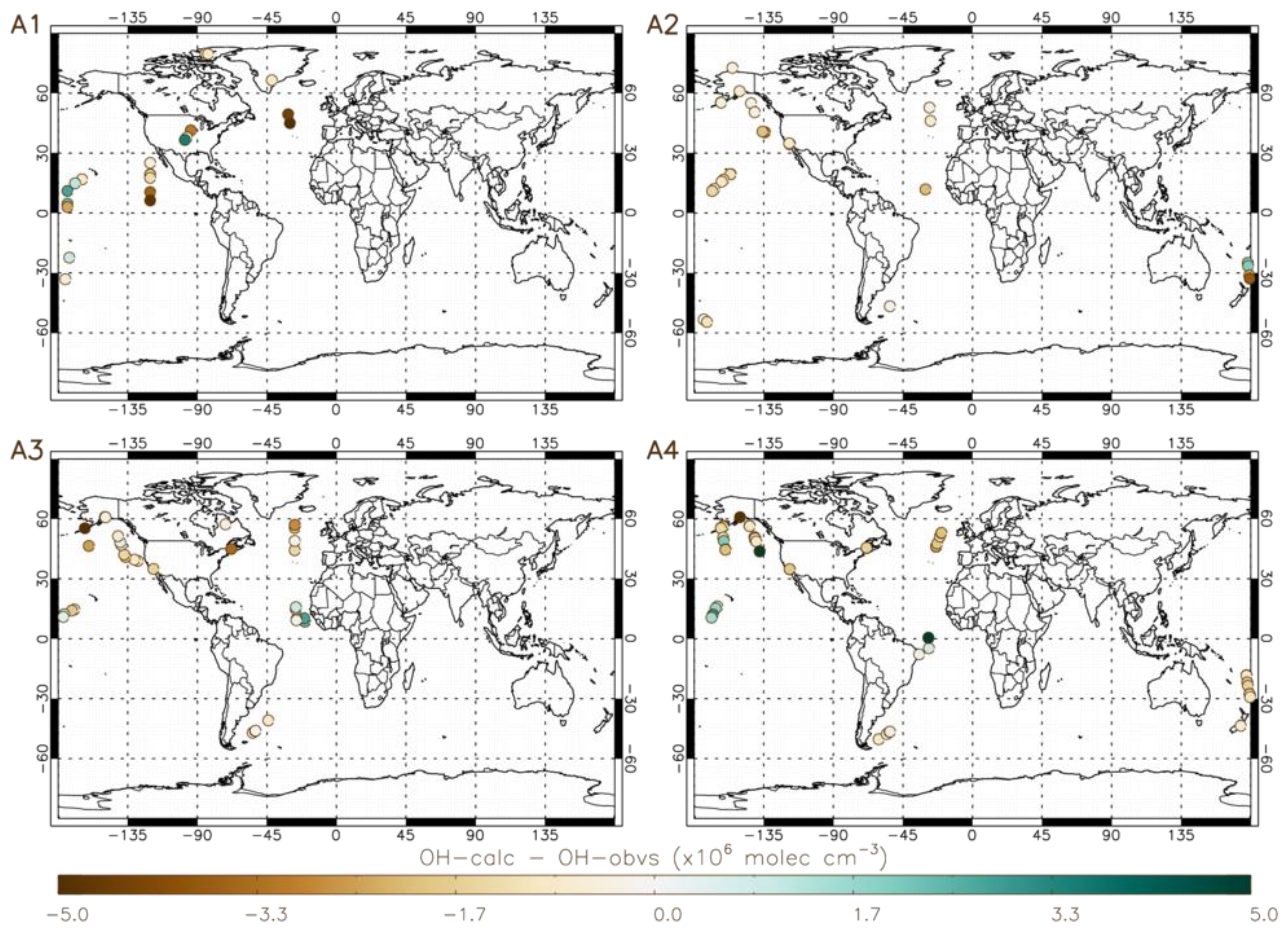


Figure R2: Difference between ATom OH-calc and OH-obvs in campaigns A1 to A4 (ATom-1 to ATom-4, 2016-2018). ATom observations are filtered for 600–700 hPa and 08:00–11:00 LT.

References

Lelieveld, J., Gromov, S., Pozzer, A. and Taraborrelli, D.: Global tropospheric hydroxyl distribution, budget and reactivity, *Atmos. Chem. Phys.*, 16(19), 12477–12493, doi:10.5194/acp-16-12477-2016, 2016.

Monks, S. A., Arnold, S. R., Hollaway, M. J., Pope, R. J., Wilson, C., Feng, W., Emmerson, K. M., Kerridge, B. J., Latter, B. L., Miles, G. M., Siddans, R. and Chipperfield, M. P.: The TOMCAT global chemical transport model v1.6: Description of chemical mechanism and model evaluation, *Geosci. Model Dev.*, doi:10.5194/gmd-10-3025-2017, 2017.

Munro, R., Lang, R., Klaes, D., Poli, G., Retscher, C., Lindstrot, R., Huckle, R., Lacan, A., Grzegorski, M., Holdak, A., Kokhanovsky, A., Livschitz, J. and Eisinger, M.: The GOME-2 instrument on the Metop series of satellites: Instrument design, calibration, and level 1 data processing - An overview, *Atmos. Meas. Tech.*, 9(3), 1279–1301, doi:10.5194/amt-9-1279-2016, 2016.

Naik, V., Voulgarakis, A., Fiore, A. M., Horowitz, L. W., Lamarque, J. F., Lin, M., Prather, M. J., Young, P. J., Bergmann, D., Cameron-Smith, P. J., Cionni, I., Collins, W. J., Dalsøren, S. B., Doherty, R., Eyring, V., Faluvegi, G., Folberth, G. A., Josse, B., Lee, Y. H., MacKenzie, I. A., Nagashima, T., Van Noije, T. P. C., Plummer, D. A., Righi, M., Rumbold, S. T., Skeie, R., Shindell, D. T., Stevenson, D. S., Strode, S., Sudo, K., Szopa, S. and Zeng, G.: Preindustrial to present-day changes in tropospheric hydroxyl radical and methane lifetime from the Atmospheric Chemistry and Climate Model Intercomparison Project (ACCMIP), *Atmos. Chem. Phys.*, 13(10), 5277–5298, doi:10.5194/acp-13-5277-2013, 2013.

Prinn, R. G., Huang, J., Weiss, R. F., Cunnold, D. M., Fraser, P. J., Simmonds, P. G., McCulloch, A., Harth, C., Salameh, P., O'Doherty, S., Wang, R. H. J., Porter, L. and Miller, B. R.: Evidence for substantial variations of atmospheric hydroxyl radicals in the past two decades, *Science* (80-), 292(5523), 1882–1888, doi:10.1126/science.1058673, 2001.

Rowlinson, M. J., Rap, A., Arnold, S. R., Pope, R. J., Chipperfield, M. P., McNorton, J., Forster, P., Gordon, H., Pringle, K. J., Feng, W., Kerridge, B. J., Latter, B. L. and Siddans, R.: Impact of El Niño Southern Oscillation on the interannual variability of methane and tropospheric ozone, *Atmos. Chem. Phys. Discuss.*, 2, 1–20, doi:10.5194/acp-2019-222, 2019.

Shetter, R. E. and Müller, M.: Photolysis frequency measurements using actinic flux spectroradiometry during the PEM-Tropics mission: Instrumentation description and some results, *J. Geophys. Res. Atmos.*, 104(D5), 5647–5661, doi:10.1029/98JD01381, 1999.

Spivakovsky, C. M., Logan, J. A., Montzka, S. A., Balkanski, Y. J., Foreman-Fowler, M., Jones, D. B. A., Horowitz, L. W., Fusco, A. C., Brenninkmeijer, C. A. M., Prather, M. J., Wofsy, S. C. and McElroy, M. B.: Three-dimensional climatological distribution of tropospheric OH: Update and evaluation, *J. Geophys. Res. Atmos.*, 105(D7), 8931–8980, doi:10.1029/1999JD901006, 2000.

Stone, D., Whalley, L. K. and Heard, D. E.: Tropospheric OH and HO₂ radicals: Field measurements and model comparisons, *Chem. Soc. Rev.*, 41(19), 6348–6404, doi:10.1039/c2cs35140d, 2012.

Voulgarakis, A., Marlier, M. E., Faluvegi, G., Shindell, D. T., Tsigaridis, K. and Mangeon, S.: Interannual variability of tropospheric trace gases and aerosols: The role of biomass burning emissions, *J. Geophys. Res. Atmos.*, 120, 7157–7173, doi:<http://dx.doi.org/10.1002/2014JD022926>, 2015.

Wofsy, S. C., Afshar, S., Allen, H. M., Apel, E., Asher, E. C., Barletta, B., Bent, J., Bian, H., Biggs, B. C., Blake, D. R., Blake, N., Bourgeois, I., Brock, C. A., Brune, W. H., Budney, J. W., Bui, T. P., Butler, A., Campuzano-Jost, P., Chang, C. S., Chin, M., Commane, R., Correa, G., Crounse, J.

D., Cullis, P. D., Daube, B. C., Day, D. A., Dean-Day, J. M., Dibb, J. E., Di Gangi, J. P., Diskin, G. S., Dollner, M., Elkins, J. W., Erdesz, F., Fiore, A. M., Flynn, C. M., Froyd, K., Gesler, D. W., Hall, S. R., Hanisco, T. F., Hannun, R. A., Hills, A. J., Hints, E. J., Hoffman, A., Hornbrook, R. S., Huey, L. G., Hughes, S., Jimenez, J. L., Johnson, B. J., Katich, J. M., Keeling, R. F., Kim, M. J., Kupc, A., Lait, L. R., Lamarque, J.-F., Liu, J., McKain, K., McLaughlin, R. J., Meinardi, S., Miller, D. O., Montzka, S. A., Moore, F. L., Morgan, E. J., Murphy, D. M., Murray, L. T., Nault, B. A., Neuman, J. A., Newman, P. A., Nicely, J. M., Pan, X., Paplawsky, W., Peischl, J., Prather, M. J., Price, D. J., Ray, E., Reeves, J. M., Richardson, M., Rollins, A. W., Rosenlof, K. H., Ryerson, T. B., Scheuer, E., Schill, G. P., Schroder, J. C., Schwarz, J. P., St. Clair, J. M., Steenrod, S. D., Stephens, B. B., Strode, S. A., Sweeney, C., Tanner, D., Teng, A. P., Thames, A. B., Thompson, C. R., Ullmann, K., Veres, P. R., Vieznor, N., Wagner, N. L., Watt, A., Weber, R., Weinzierl, B., et al.: ATom: Merged Atmospheric Chemistry, Trace Gases, and Aerosols, ORNL Distrib. Act. Arch. Cent., doi:10.3334/ORNLDaac/1581, 2018.